www.czasopisma.pan.pl PAN POLSKA AKADEMIA NAUK www.journals.pan.pl

Arch. Metall. Mater. **67** (2022), 2, 773-778

DOI: https://doi.org/10.24425/amm.2022.137817

R. KOSTUREK[1*], L. ŚNIEŻEK[1], K. GRZELAK[1], M. WACHOWSKI[1]

RESEARCH ON THE MICROSTRUCTURE OF LASER BEAM WELDED SC-MODIFIED AA2519-F EXTRUSION

In this paper, the microstructure of laser beam welded Sc-modified AA2519-F has been taken under investigation. The welded joint has been produced using Fanuc 710i industrial robot equipped with YLS-6000 6 kW laser beam source. The welding speed and laser power were equal to 0.75 m/min and 3.2 kW, respectively. The investigation involved microstructure observations with the use of both light microscope and scanning electron microscope with energy dispersive spectroscopy (EDS) analysis of chemical composition and microhardness distribution measurements. It has been stated that laser beam welding allows to obtain Sc-modified AA2519-F weld of good quality, characterized by the presence of an equiaxed grain zone containing scandium-rich precipitates adjacent to the fusion boundary.

Keywords: aluminum; extrusion; AA2519; microstructure; laser beam welding

1. Introduction

In many cases, a wider application of construction material is often limited by the accessibility of its welding technology and equipment [1,5]. A good example of such materials are 2XXX aluminum alloys, especially these characterized by a relatively high concentration of copper – 2219 and 2519 [6,7]. Their high specific strength contributed to their application in lightweight structures, e.g. aircraft components and light military vehicles [8]. In recent publications, we have shown that involving new, advanced welding techniques (e.g. *friction stir welding*) allows to overcome several problems typical for joining AA2519 alloy by conventional means (*hot cracking, pores)* [9,10]. A noteworthy fact is that AA2519 modified by the addition of scandium has been developed in the past year by the Institute of Non-Ferrous Metals, Light Metals Division in Skawina [11]. Scandium not only provides higher strength of the alloy and increases the recrystallization temperature but also causes a grain refinement during the solidification of modified AA2519 [12-14]. Due to this phenomenon, scandium can play a very profitable role in the welding process and is used as an alloying element in some filler wires [15,16]. Considering the conventional welding techniques of aluminum alloys - tungsten inert gas (TIG) or metal inert gas (MIG), it can be stated that both are characterized by significant heat input and relatively wide welds [17-22]. For these reasons, the laser beam welding technique is far more effective, allowing to notably reduce the affecting of temperature on the welded workpieces, providing highly localized melting of material [23]. Although, joints produced by laser beam welding of various aluminum alloys have been subjects of many investigations in recent years, the properties of Sc-modified 2XXX alloy welds are still a major gap in the current state of the art.

2. Experimental procedure

The material to be weld was 5 mm thick AA2519-F extrusion with dimensions of 80×250 mm. The chemical composition of the alloy and its mechanical properties are presented in TABLE 1 and 2 respectively.

TABLE 1

Chemical composition of AA2519 [% weight]

Fe	Si	Cu	Zn	Ti	Mn	Mg	Ni	Zr	Sc	V	Al
0.11	0.08	6.32	0.05	0.08	0.17	0.33	0.02	0.19	0.16	0.10	Base

TABLE 2

Mechanical properties of AA2519-F

Young Modulus (E)	Yield Strength ($R_{e0,2}$)	Tensile Strength (R_m)	Elongation (A)
67 GPa	291 MPa	334 MPa	7 %

[1] MILITARY UNIVERSITY OF TECHNOLOGY, FACULTY OF MECHANICAL ENGINEERING, 2 GEN. S. KALISKIEGO STR., 00-908 WARSZAWA, POLAND

* Corresponding author: robert.kosturek@wat.edu.pl

The initial state of the material to be weld was as-extruded (non-heat treated) with the measured value of microhardness equal 90-95 HV0.1. Before the welding the workpiece have been ground and cleaned with isopropyl alcohol. The welded joint has been produced using Fanuc 710i industrial robot equipped with YLS-6000 6 kW laser beam source. The chosen type of laser (Nd:YAG) provides better processing efficiency compared to CO_2 laser with the same power and enhanced coupling into reflective materials, what increases the weldability of aluminum. The selection of welding parameters based on our experience and optimization in the wide range of parameters (laser power range: 2.9-3.8 kW, welding velocity range: 0.5-2 m/min).

The welding parameters have been set in TABLE 3. The laser beam has been focused on the workpiece surface.

TABLE 3

The used parameters of laser beam welding

Laser power	Welding speed	Laser beam width	Laser beam inclination angle	Shielding gas	Shielding gas flow
3.2 kW	0.75 m/min	0.2 mm	10°	Argon	10 L/min

The sample for microstructure investigation has been cut perpendicular to the welding direction (cross-weld) then prepared according to the standard metallographic techniques for specimen preparation. The microstructure has been revealed using Kroll reagent (20 mL H_2O + 5 mL HNO_3 + 1 mL HF) with an etching time equal to 5 s. The microstructure observations have been performed using a digital light microscope Olympus LEXT OLS 4100 and scanning electron microscope (SEM) Jeol JSM-6610. The Vickers microhardness has been measured on the cross-section of the polished sample by applying a load of 0.98 N according to EN ISO 6507 standard. The microhardness distribution has been performed for three lines at a distance of 0.5, 2.5, and 4.2 mm from the top of the sample.

3. Results and discussion

The microstructure of the base material is presented in Fig. 1. The base material is characterized by significant differences in the grain size (Fig. 1a) and Al_2Cu precipitates (Fig. 1b). The performed observations of the obtained welded sample (Fig. 2) allow to state that the joint is of good quality. It is characterized by the presence of porosity (about 0.4 mm size) in the bottom part of the joint and excessive root penetration with its high of 0.8 mm. The rounded shape of the porosity, suggests originating from gasses. At the same time, no presence of cracks has been reported on the macroscopic level. The width of the weld is far more lower compared to welds obtained by TIG or MIG technique, as a result of the smaller melted pool [24].

The results of microhardness measurements (Fig. 3) show that laser beam welding causes significant changes in the hardness of welded alloy especially when it comes to the heat-affected zone.

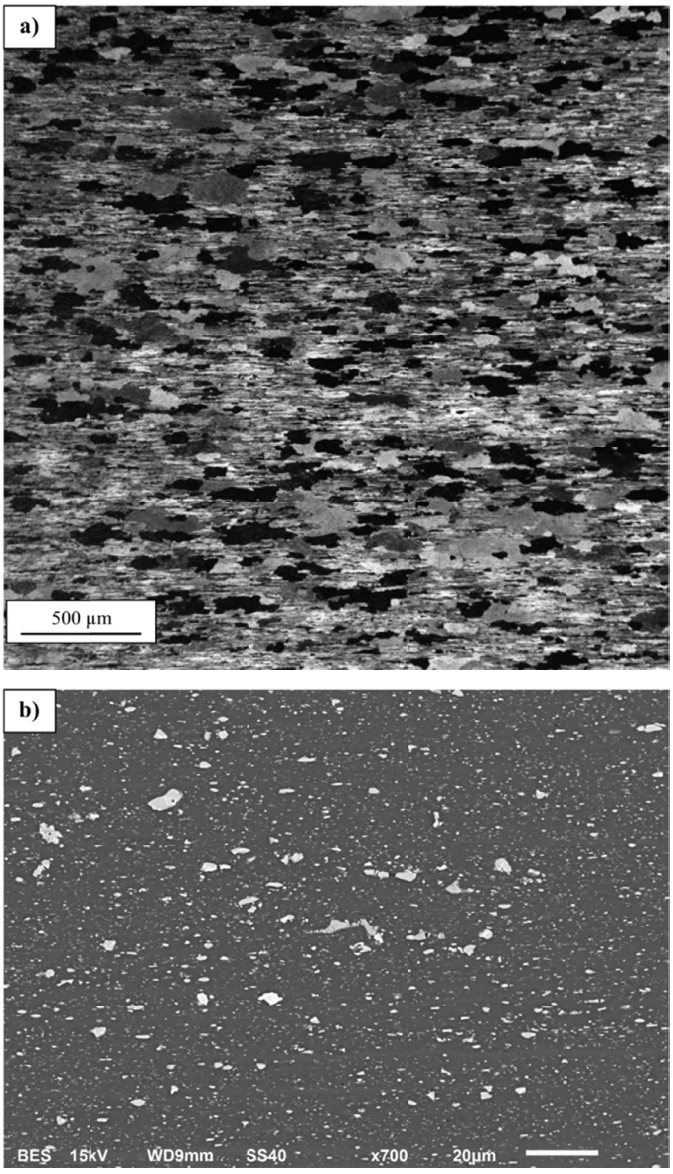

Fig. 1. The microstructure of the base material: a) grains (light microscope), b) distribution of Al_2Cu precipitates (SEM)

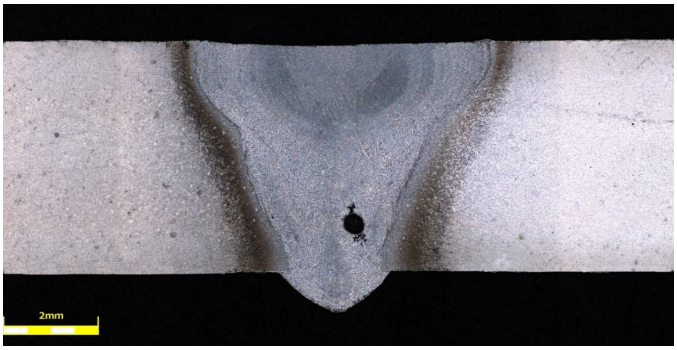

Fig. 2. The macrostructure of the welded joint

The microhardness of base material predominantly contains within the range of 90-95 HV0.1. The spreads of microhardness are expected in the case of AA2519 for its high copper concentration (6.3% Cu) results in the presence of large Al_2Cu precipitates

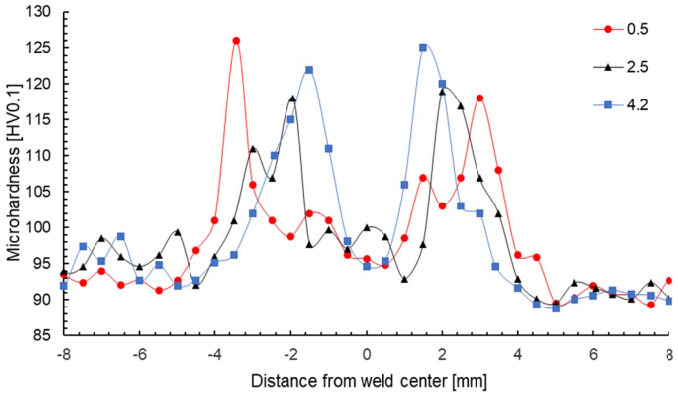

Fig. 3. The microhardness distribution on the weld cross-section at a distance of 0.5, 2.5, and 4.2 mm from the top of the sample

[9]. The obtained distribution partly reflects the macrostructure with the upper (0.5 mm), middle (2.5 mm), and bottom (4.2) part of the weld having established the width of fusion zone equal to 6, 4, and 3 mm respectively. The highest values of microhardness (about 120-125 HV0.1) have been reported in the immediate vicinity of the fusion boundary for all three investigated lines. From these points, it can be observed, that the microhardness decreases to the center of the joint, where it reaches a value of 90-95 HV0.1 (corresponding to the base materials value). In the next part of the investigation the grainy microstructure of the weld has been subjected to the analysis (Fig. 4a-d).

The zone adjacent to the fusion boundary consists of fine, equiaxed grains (Fig. 4a) formed as a result of the heterogeneous nucleation of new grains at the fusion boundary [23]. The size

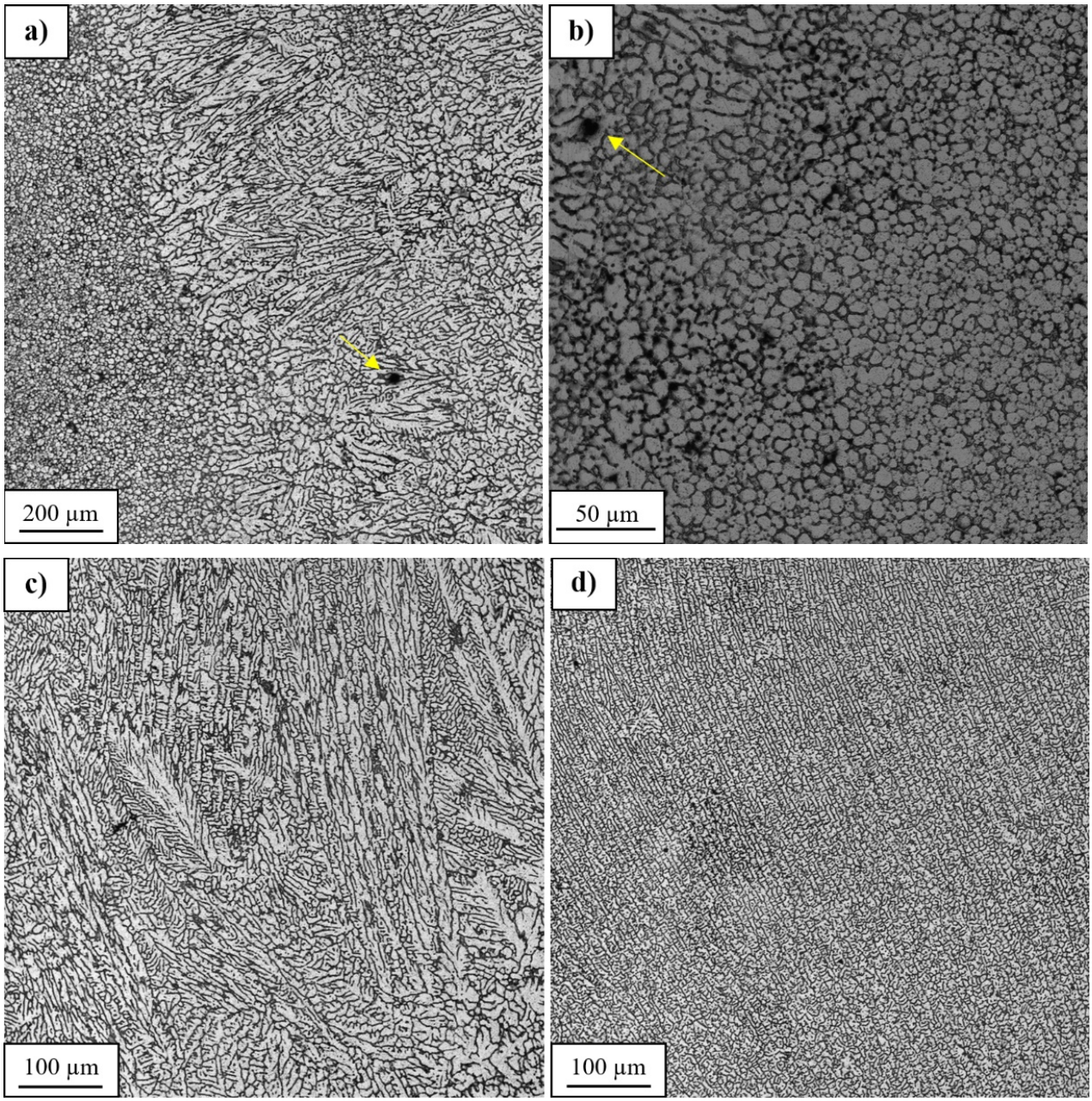

Fig. 4. The microstructure of weld: a) equiaxed grains and columnar dendrites interface, b) equiaxed grain zone, c) columnar dendrites, d) equiaxed dendrites. Pores marked with yellow arrows

of grains is mostly about 10 μm, but even grains of smaller size (3-5 μm) can be found closer to the fusion boundary (Fig. 4b). The formation of equiaxed grain zone occurs in temperature range 630-640°C [25] and it is strongly related to the composition of the welded material [23]. Alloying elements such as Zr and Sc form fine dispersoids, which supports the nucleation and growth of new grains [25]. Following the gradient of the heat flow, the columnar dendrite zone can be distinguished next to the equiaxed grain zone (Fig. 4a). Despite the fact that the size and shape of dendrites differ in a different part of the weld, they are always oriented in accordance with the heat flow, analogously to the columnar grains in the as-cast microstructure in conventional welding processes (Fig. 4c). The center part of the weld is characterized by the microstructure consisting of equiaxed dendrites (Fig. 4d). Additionally, during the microstructure examination the sporadic occurrence of shrinkage-related pores has been reported, (mostly in areas close to the fusion boundary), but their size was relatively small and in most cases did not exceed 10 μm (Fig. 4b). The performed microscopic observations did not reveal the presence of cracks in the investigated sample. The area consisting of equiaxed grains and columnar dendrites (Fig. 4a) has been subjected to further analysis with the use of the scanning electron microscope. The SEM image allows to observe the interdendritic segregation of heavy elements (Cu) in the form of Al_2Cu precipitates in the investigated area (Fig. 5).

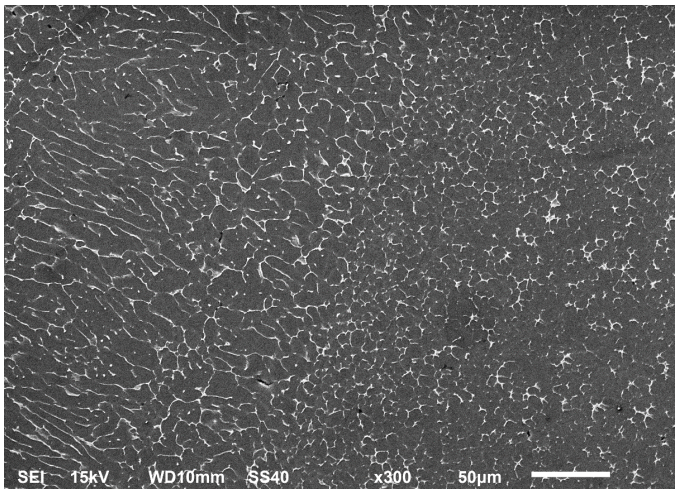

Fig. 5. The distribution of Al_2Cu intermetallic precipitates in the zone adjacent to the fusion boundary

The distribution of the intermetallic precipitates partly corresponds to the previous observations of the weld grainy microstructure (Fig. 4a). The finest precipitates are localized in the equiaxed grain zone and it is possible to observe the partly melted zone characterized by the presence of small, unregular dendrites. Comparing the results of microhardness distribution and microstructure observation it can be stated that the formation of ultrafine, equiaxed grains and precipitates is the reason for the high values of microhardness (120-125 HV0.1). In order to investigate the chemical composition of this zone, the EDS analysis has been carried out (Fig. 6).

The chemical composition analysis has been performed in 4 different points marked on Fig. 6. The results indicate on predominant concentration of aluminum (60-70%) and copper (30-40%) and elevated concentrations of iron (about 0.5%) and scandium (0.2-0.6%) in the interdendritic precipitates. At the same time, the concentration of elements in the dendrite cores shows high concentration of aluminum (98%) and relatively low concentration of copper (2%) corresponding to the basic, saturated solid solution of Cu in Al. It has been reported that interdendritic areas have noticeable participation of micropores, formed during solidification of Al_2Cu precipitates (Fig. 6).

4. Conclusions

The performed investigation on the microstructure of Sc-modified AA2519-F laser beam welded joint allows the following conclusion to be drawn:

1. The used welding parameters (power of 3.2 kW and welding velocity of 0.75 m/min) allowed to produce the joint of good quality with low participation of pores and without cracks.
2. The area adjacent to the fusion boundary has been identified as the equiaxed grain zone, characterized by high microhardness (120-125 HV0.1) and the presence of ultrafine, equiaxed grains with their size predominantly about 10 μm.
3. The SEM observation revealed the interdendritic segregation of Al_2Cu precipitates with micropores. Additionally, the interdendritic precipitates have slightly elevated concentrations of iron and scandium.

Acknowledgements

This research was funded by Polish Ministry of National Defence, grant number: PBG/13-998.

REFERENCES

[1] V. Hutsaylyuk, M. Student, V. Dovhunyk, V. Posuvailo, O. Student, P. Maruschak, I. Koval'chuck, Metals **9**, 280 (2019). DOI: https://doi.org/110.3390/met9030280

[2] R. Kosturek, M. Wachowski, L. Śnieżek, A. Kruk, J. Torzewski, K. Grzelak, J. Mierzyński, Materiali in Tehnologije **53**, 109-113 (2019). DOI: https://doi.org/110.17222/mit.2018.153

[3] A. Guzanová, J. Brezinová, D. Draganovská, P.O. Maruschak, Koroze a Ochrana Materialu **63**, 86-93 (2019).

[4] R. Kosturek, M. Wachowski, L. Śnieżek, M. Gloc, Metals **9**, 1-16 (2019). DOI: https://doi.org/110.3390/met9020246

[5] R. Kosturek, M. Najwer, P. Niesłony, M. Wachowski, Lecture Notes in Mechanical Engineering **201519**, 681-686 (2018). DOI: https://doi.org/110.1007/978-3-319-68619-6_65

[6] M. Wachowski, R. Kosturek, L. Śnieżek, S. Mróz, M. Gloc, A. Krawczyńska, M. Małek, Materiali in Tehnologije **53**, 239-243 (2019). DOI: https://doi.org/110.17222/mit.2018.151

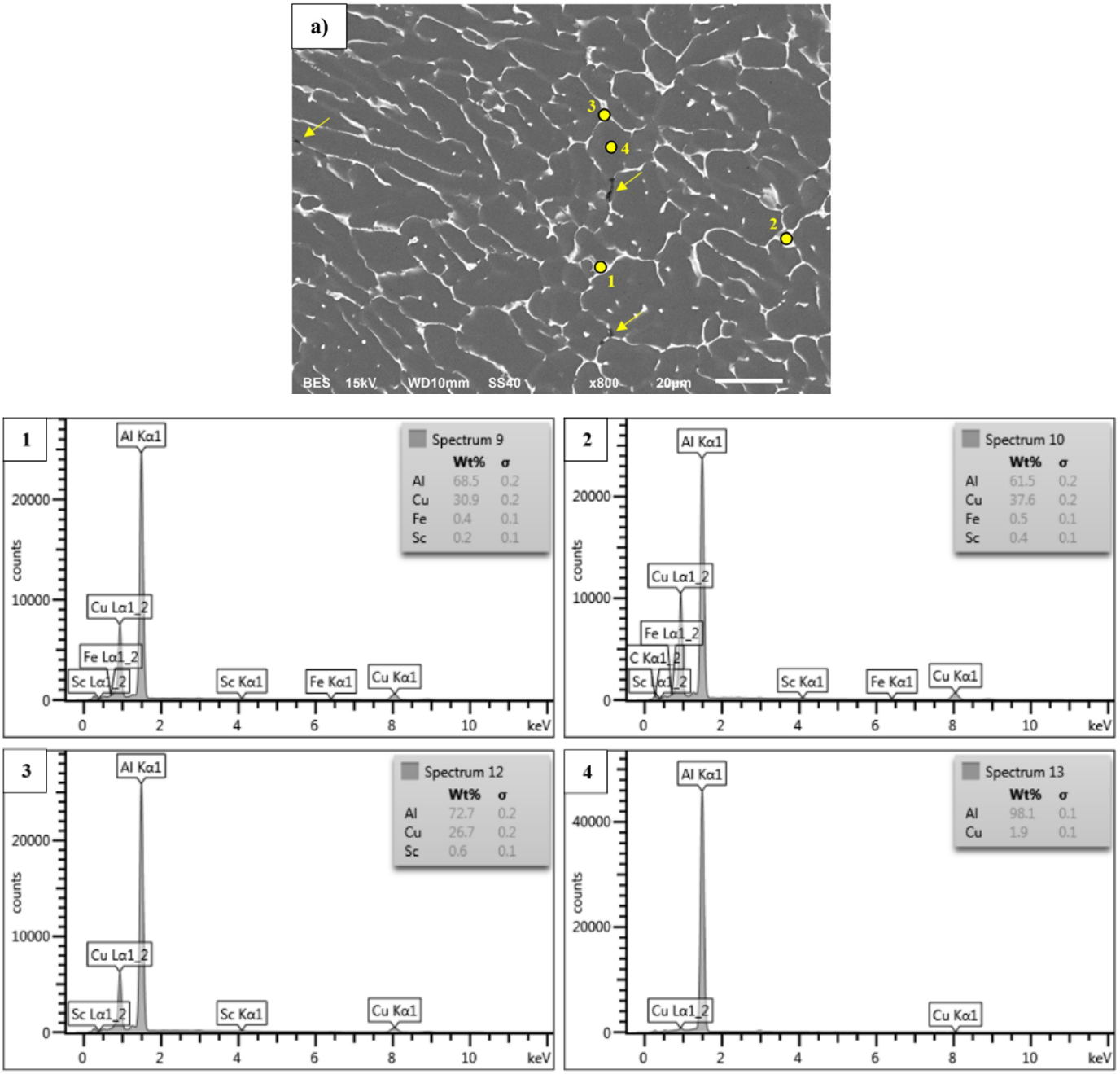

Fig. 6. The equiaxed grains and columnar dendrites interface a) the analyzed zone 1-4) the results chemical composition analysis. Pores marked with yellow arrows

[7] C. Chen, M. Gao, H. Mu, X. Zeng, J. Laser Appl. **31**, 032005 (2019). DOI: https://doi.org/110.2351/1.5094804

[8] V. Hutsaylyuk, M. Student, V. Posuvailo, O. Student, Y. Sirak, V. Hvozdets'kyi, P. Maruschak, H. Veselivska, Vaccum **179**, 109514 (2020).

[9] R. Kosturek, L. Śnieżek, J. Torzewski, M. Wachowski, Metals **9**, 1-15 (2019). DOI: https://doi.org/110.3390/met9101024

[10] R. Kosturek, L. Śnieżek, J. Torzewski, M. Wachowski, Manufacturing Review **7**, 28 (2020). DOI: https://doi.org/110.1051/mfreview/2020025

[11] B. Płonka, M. Rajda, Z. Zamkotowicz, J. Zelechowski, K. Remsak, P. Korczak, W. Szymański, L. Śnieżek, Arch. Metal.l Mater. **61**, 381-388 (2016). DOI: https://doi.org/110.1515/amm-2016-0070

[12] Y. Liu, C. Zhang, X. Zhang, Y. Huang, Intermetallics **123**, 106823 (2020). DOI: https://doi.org/110.1016/j.intermet.2020.106823

[13] A. Smolej, B. Markoli, A. Nagode, D. Klobčar, RMZ-Materials and Geoenvironment **62**, 73-80 (2015).

[14] R. Guan, D. Tie, Acta Metallurgica Sinica (English Letters) **30** (2017). DOI: https://doi.org/110.1007/s40195-017-0565-8

[15] Z. Silvayeh, R. Vallant, C. Sommitsch et al., Metall. Mater. Trans. A **48**, 5376-5386 (2017). DOI: https://doi.org/110.1007/s11661-017-4277-5

[16] A.F. Norman, S.S. Birley, P.B. Prangnell, Sci. Technol. Weld. Joi. **8**, 235-245 (2003). DOI: https://doi.org/110.1179/136217103225010989

[17] J. Viňáš, J. Brezinová, J. Brezina, P.O. Maruschak, Mater. Sci. **55**, 46-51 (2019). DOI: https://doi.org/110.1007/s11003-019-00250-x

[18] G. Rogalski, A. Świerczyńska, M. Landowski, D. Fydrych, Metals **10**, 559 (2020).

[19] J. Winczek, J. Iwaszko, M. Matuszewski, IOP Conference Series: Materials Science and Engineering **776**, 012056 (2020). DOI: https://doi.org/110.1088/1757-899X/776/1/012056

[20] J. Górka, M. Przybyła, M. Szmul, A. Chudzio, D. Ładak, Adv. Mater. Res.-Switz. **19**, 55-64 (2019). DOI: https://doi.org/110.2478/adms-2019-0017

[21] G. Rogalski, A. Swierczynska, D. Fydrych, M. Landowski, Welding Technology Review **91** (2019). DOI: https://doi.org/110.26628/wtr.v91i4.1017

[22] D. Rozumek, J. Lewandowski, G. Lesiuk, J. Correia, Int. J. of Fatigue **131**, 105328 (2020). DOI: https://doi.org/110.1016/j.ijfatigue.2019.105328

[23] N. Kashaev, V. Ventzke, G. Çam, J. Manuf. Process **36**, 571-600 (2018). DOI: https://doi.org/110.1016/j.jmapro.2018.10.005

[24] C. Yeni, S. Sami, M. Pakdil, Kovove Materialy **47**, 341-347 (2009).

[25] D.C. Lin, G. Wang, T. Srivatsan, Materials Science and Engineering: A **351**, 304-309 (2003). DOI: https://doi.org/110.1016/S0921-5093(02)00858-4